



## MULTIPLE REFERENCE FEEDFORWARD ACTIVE NOISE CONTROL PART II: REFERENCE PREPROCESSING AND EXPERIMENTAL RESULTS

Y. TU AND C. R. FULLER

*Vibration and Acoustic Laboratories, Mechanical Engineering Department, Virginia  
Polytechnic Institute and State University, Blacksburg, VA 24061-0238, U.S.A.*

*(Received 6 June 1997, and in final form 13 November 1998)*

Multiple reference active noise control (MRANC) has been applied to acoustical fields with multiple noise sources to achieve low frequency noise reduction. The traditional control configuration feeds each reference signal into a different control filter. This configuration has been widely adopted due to its potential performance in a general multiple noise source environment. However, it entails the problem of ill conditioning when the reference signals are correlated. In this paper time domain analysis has been carried out to investigate the problem of ill conditioning for MRANC. To cope with the problem of ill conditioning, a reference signal preprocessing step is added to the conventional active noise control process. This preprocessing step essentially constructs a new set of reference signals, which preserve all the information of the original reference, but are uncorrelated with each other. An adaptive decorrelation filter based on the Wiener filter theory and Gram–Schmidt orthogonalization theorem is constructed to implement the reference signal preprocessing step. Experiments based on sound transmission through a vibrating plate have been conducted and the results presented are consistent with the theoretical analysis.

© 2000 Academic Press

### 1. INTRODUCTION

With the breathtaking advance of digital signal processing (DSP) technology and ever-increasing parallelism for real-time computation, complex feedforward active noise control (ANC) systems with multiple reference, multiple actuator and multiple error have been built. These complex ANC systems make noise reduction possible not only in single noise source one-dimensional acoustical fields, but in multiple noise source three-dimensional acoustical fields as well. When an ANC system is applied to a three-dimensional acoustical field, it is usually required to use multiple actuator and multiple error sensor to achieve spatial noise reduction [1].

In addition, to achieve noise reduction in a multiple noise source environment, it is usually required to use an array of reference sensors to generate a complete set of reference signals [2] so that the desired multiple coherence function can be obtained. A previous companion paper [3] studied the behavior of conventional and simplified multiple reference active noise control (MRANC) systems using frequency domain analysis and simulation. It was found that good performance in terms of noise reduction could be achieved with the conventional configuration, and a simplified configuration is possible under some special circumstances. Over the years, many different schemes and devices have been investigated in an effort to minimize the number of reference sensors

while achieving maximum noise reduction. It has also been realized that, if the reference signals are correlated, the MRANC system may become ill conditioned which usually results in a slow convergence rate and high sensitivity of noise attenuation to the measurement contamination.

A method to increase the convergence speed by using decorrelators for a MRANC system was proposed by Masato *et al.* [4]. The effectiveness of the proposed decorrelators to increase convergence speed is strongly affected by the characteristics of the reference signal correlation. In a general situation, the proposed decorrelators deliver poor results. Studies on adaptive noise cancellation, in which the cancellation is focused on electrical signals rather than acoustical waves, have shown that the reference signal coupling in a multiple noise source environment degrades the control performance. A decoupling method was proposed to produce a new set of reference signals [5]. Parallel adaptive filter structures along with sub-band approaches have also been applied to adaptive noise cancellation. The results are shown to improve the ability to track non-stationary noise process [6]. Recently, attention has been paid to the convergence rate as well as the number of control coefficients for reference sensor selection [7] in a multiple noise source environment.

The previous studies on MRANC are mainly focused on noise source identification and reference sensor selection. An important issue remains unsolved, i.e., when reference signals are correlated, the ANC system becomes ill-conditioned. An ill-conditioned system usually results in slow convergence rate and high sensitivity of noise attenuation to measurement contamination. In this paper, the problem of ill conditioning has been analytically studied using a time domain analysis. A reference signal preprocessing step using adaptive decorrelation filters is proposed and investigated using simulations and experiments. It is shown that the preprocessing step significantly improves the performance of the MRANC system when the reference signals are correlated.

## 2. TIME DOMAIN ANALYSIS

Figure 1 shows a typical MRANC system, in which there are  $M$  noise sources,  $K$  reference sensors, one secondary source and one error sensor. Each reference signal is fed into a different filter and the output of each filter is summed together to drive a single secondary source. This structure for processing reference signals attempts to control the primary noise from multiple primary paths with the secondary noise from multiple filters, thus it enjoys the applicability in general situations and has been adopted by most previous studies [2, 8]. Since the number of the secondary sources and error sensors is chosen to be unity to simplify the analysis, the spatial noise reduction effect is not a concern in this paper.

Usually, reference signals are obtained through various sensors, and each reference sensor may pick up signals from several noise sources passing through different paths, as shown in Figure 2. As a result, the reference signals may be correlated with each other. The correlated part of these reference signals represents the common input to different filters, which in turn generates the correlated outputs. The error signal at step  $k$  can be written as

$$e(k) = d(k) + u(k)T(z), \quad (1)$$

where  $T(z)$  is the  $Z$  transform of the error path. Here, no assumption is made about the structure of  $T(z)$ , it could be in the form of either IIR or FIR filters, and  $u(k)$  is the summation of all the filter outputs, given by

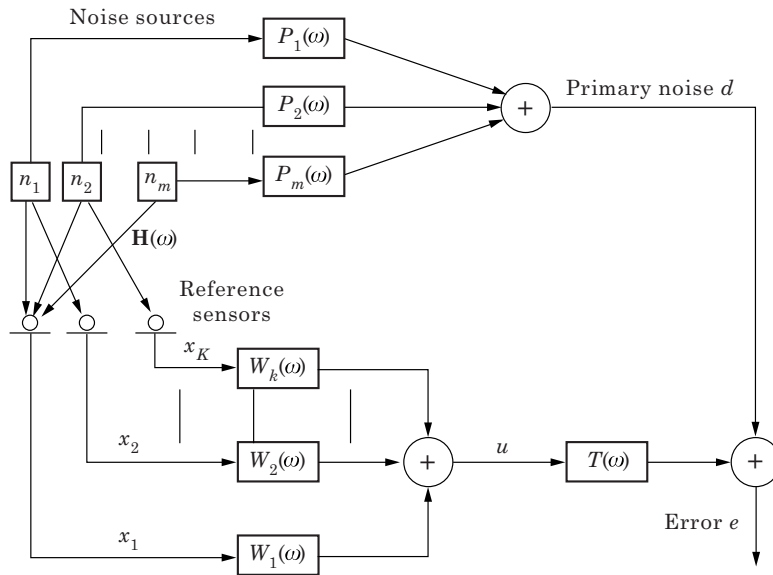


Figure 1. Multiple reference multiple input (MRMI) system.

$$u(k) = \sum_{i=1}^K \mathbf{x}_i^T(k) \mathbf{w}_i = \sum_{i=1}^K \mathbf{w}_i^T \mathbf{x}_i(k), \tag{2}$$

where  $\mathbf{w}_i$  and  $\mathbf{x}_i(k)$  are the weight vector and the tapped input vector for the  $i$ th filter, respectively. Suppose the filter length is  $N$ , then

$$\mathbf{w}_i = [w_{0,i} \quad w_{1,i} \quad w_{2,i} \cdots w_{N-1,i}]^T, \tag{3}$$

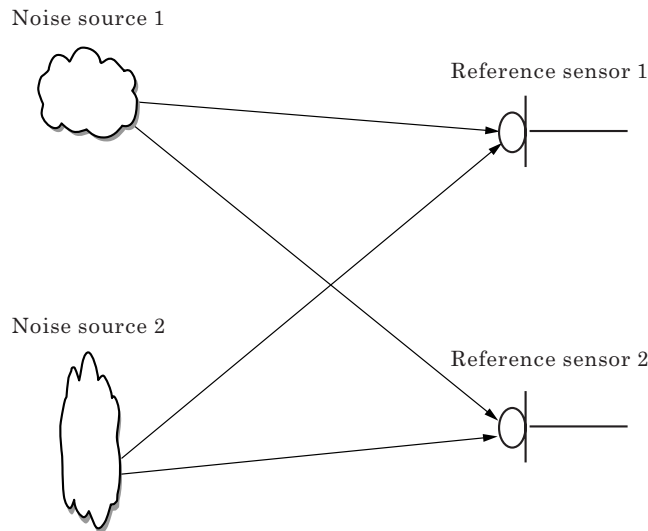


Figure 2. Noise sources and reference sensors.

$$\mathbf{x}_i(k) = [x_i(k)x_i(k-1) \cdots x_i(k-N+1)]^T. \quad (4)$$

Substituting equation (2) into equation (1) yields

$$e(k) = d(k) + \sum_{i=1}^K \mathbf{w}_i^T(k)T(z). \quad (5)$$

Defining the filtered reference signal as

$$\hat{\mathbf{x}}_1(k) = \mathbf{x}_i(k)T(z), \quad (6)$$

the error signal can be rewritten as

$$e(k) = d(k) + \mathbf{W}^T \hat{\mathbf{X}}(k), \quad (7)$$

where  $\mathbf{W}$  is a  $K \times N$  vector formed by putting together all the control filter weight vectors and  $\hat{\mathbf{X}}(k)$  is another  $K \times N$  vector formed by putting together all the reference signal vectors, i.e.,

$$\mathbf{W} = (\mathbf{w}_1^T \quad \mathbf{w}_2^T \cdots \mathbf{w}_k^T)^T, \quad \hat{\mathbf{X}}(k) = (\hat{\mathbf{x}}_1^T(k)x_2^T(k) \cdots \hat{\mathbf{x}}_k^T(k))^T. \quad (8, 9)$$

The cost function is constructed as the mean square error signal, i.e.,

$$\xi = E[e^2(k)]. \quad (10)$$

Substituting equation (5) into equation (10), the gradient of the cost function with respect to the weight vector is obtained as

$$\nabla = \frac{\partial \xi}{\partial \mathbf{W}} = 2E \left[ e(k) \frac{\partial e(k)}{\partial \mathbf{W}} \right] = 2E[d(k)\hat{\mathbf{X}}(k)] + 2E[\hat{\mathbf{X}}(k)\hat{\mathbf{X}}^T(k)]\mathbf{W}.$$

Setting the gradient to zero, the optimum weight vector is obtained by solving the norm equation

$$\mathbf{R}\mathbf{W}_{opt} = -\mathbf{P}, \quad (11)$$

where

$$\mathbf{R} = E \begin{pmatrix} \hat{x}_1(k)\hat{x}_1^T(k) & \hat{x}_1(k)\hat{x}_2^T(k) & \cdots & \hat{x}_1(k)\hat{x}_k^T(k) \\ \hat{x}_2(k)\hat{x}_1^T(k) & \hat{x}_2(k)\hat{x}_2^T(k) & \cdots & \hat{x}_2(k)\hat{x}_k^T(k) \\ \vdots & \vdots & \ddots & \vdots \\ \hat{x}_k(k)\hat{x}_1^T(k) & \hat{x}_k(k)\hat{x}_2^T(k) & \cdots & \hat{x}_k(k)\hat{x}_k^T(k) \end{pmatrix}, \quad \mathbf{P} = E \begin{pmatrix} \hat{x}_1(k)d(k) \\ \hat{x}_2(k)d(k) \\ \vdots \\ \hat{x}_k(k)d(k) \end{pmatrix}. \quad (12, 13)$$

Each term inside the above  $\mathbf{R}$  matrix is a sub-matrix, and the matrix  $\mathbf{R}$  is real, symmetric and non-negative definite just like the  $\mathbf{R}$  matrix in a single reference ANC system. Therefore, the corresponding eigenvalues of the  $\mathbf{R}$  matrix are also non-negative and real. The characteristics of the  $\mathbf{R}$  matrix are determined by the auto-correlation and cross-correlation functions of the filtered reference signals. If all the reference signals are uncorrelated with each other, every off-diagonal terms in the  $\mathbf{R}$  matrix will be zero and every optimum weight vector,  $\mathbf{w}_1, \mathbf{w}_2, \dots$  and  $\mathbf{w}_k$ , are uncoupled. On the other hand, if the reference signals are correlated, the condition number [9] of the  $\mathbf{R}$  matrix may become large, which implies that the MRANC system is ill-conditioned. This problem

may become more prominent when each reference signal is orthogonal. In this case, the auto-correlation matrices inside the  $\mathbf{R}$  matrix are diagonal, and the condition number of the  $\mathbf{R}$  matrix is determined by only the cross-correlation functions of the filtered reference signals.

It is very important to understand *perturbation theory* [9] and its impact on the development of an algorithm to solve the norm equation (11). The perturbation theory states that if the matrix  $\mathbf{R}$  and the vector  $\mathbf{P}$  are perturbed by small amounts  $\delta\mathbf{R}$  and  $\delta\mathbf{P}$ , respectively, and if the relative perturbations,  $\|\delta\mathbf{R}\|/\|\mathbf{R}\|$  and  $\|\delta\mathbf{P}\|/\|\mathbf{P}\|$ , are both on the same order of  $\varepsilon$ , where  $\varepsilon \ll 1$ , then

$$\frac{\|\delta\mathbf{W}\|}{\|\mathbf{W}\|} \leq \varepsilon\chi(\mathbf{R}), \quad (14)$$

where  $\delta\mathbf{W}$  is the change of weight vector  $\mathbf{W}$  as a result of the perturbation from the matrix  $\mathbf{R}$  and the vector  $\mathbf{P}$ , and  $\chi(\mathbf{R})$  is the *condition number* of the matrix  $\mathbf{R}$ , and  $\|\cdot\|$  is the *norm* operator [10]. The condition number describes the ill condition of a matrix. Since the matrix  $\mathbf{R}$  is real and symmetric, it can be shown [6] that the condition number equals

$$\chi(\mathbf{R}) = \lambda_{\max}/\lambda_{\min}, \quad (15)$$

where  $\lambda_{\max}$  and  $\lambda_{\min}$  are the maximum and minimum eigenvalues of the matrix  $\mathbf{R}$ , respectively. This ratio is also commonly referred to as eigenvalue spread.

The perturbation theory states that if there are some errors in the matrix  $\mathbf{R}$  or the vector  $\mathbf{P}$  caused by measurement or some other factors, the ill condition of the correlation matrix  $\mathbf{R}$  may lead to a weight vector solution  $\mathbf{W}$  which is far from the optimum Wiener solution  $\mathbf{W}_{opt}$  due to the problem of ill condition. In other words, the ill condition of the correlation matrix  $\mathbf{R}$  causes the optimum Wiener vector to be very sensitive to various kinds of measurement contamination. The measurement contamination may result from A/D and D/A conversion, transducer error, finite precision error, non-linearity, etc.

On the other hand, the eigenvalue spread of the matrix  $\mathbf{R}$  has a significant impact on the convergence rate of an ANC system, especially when the LMS based algorithm is applied [2]. An important factor that determines the eigenvalue spread is the cross-correlation among the reference signals. The cross-correlation becomes even more dominant when each reference is an orthogonal signal. In particular, if the reference signal  $x_i$  is correlated with the reference signal  $x_j$ , the  $i$ th and  $j$ th columns in the  $\mathbf{R}$  matrix will exhibit some similarities, which results in large eigenvalue spread. Upon the extreme circumstance that any two reference signals are the same, the determinant of the matrix  $\mathbf{R}$  becomes zero, and the eigenvalue spread approaches infinity. In this case, the ill-conditioned system deteriorates to an underdetermined system since the solution to the ANC system is not unique.

### 3. PREPROCESSING OF REFERENCE SIGNALS

As discussed in the last section, it is desirable to have uncorrelated reference signals. In the present work, this is achieved with an additional reference preprocessing stage right before feeding the reference signals into controllers. The preprocessing constructs a new set of reference signals, which preserve all the information of the original reference signals, but are uncorrelated with each other. Such a step essentially causes all the off-

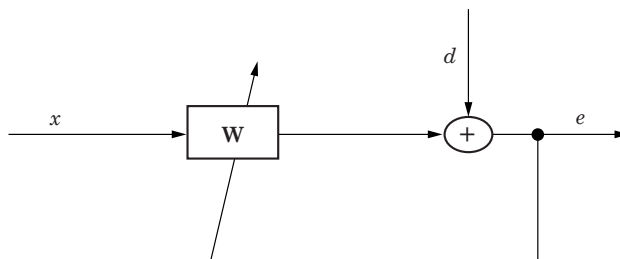


Figure 3. An adaptive transversal filter.

diagonal blocks in the  $\mathbf{R}$  matrix to be zero, thus eliminating the ill-conditioning problem due to the cross-correlation among reference signals.

According to the orthogonal theorem of adaptive filter theory, when an adaptive filter shown in Figure 3 is running as an optimum Wiener filter, the error signal is uncorrelated with the reference signal, i.e.,

$$E[x(k-i)e(k)]_{\mathbf{w}=\mathbf{w}_{opt}} = 0, \quad i = 0, 1, 2, \dots, M-1, \quad (16)$$

where  $x$  is the reference signal,  $e$  is the error signals, and  $M$  is the number of filter coefficients. Based on the orthogonal theorem, adaptive decorrelation filters can be constructed as shown in Figure 4, in which two correlated reference signals are processed by a couple of adaptive filters to generate two uncorrelated reference signals. For the upper filter  $\mathbf{A}$ , the reference signal is  $\bar{x}_1$ , and the error signal is  $\bar{x}_2$ . Thus, the orthogonal relationship is expressed as

$$E[\bar{x}_1(k-i)\bar{x}_2(k)]_{\mathbf{A}=\mathbf{A}_{opt}} = 0, \quad i = 0, 1, 2, \dots, M-1, \quad (17)$$

where  $M$  is the number of filter coefficients corresponding to filter  $\mathbf{A}$ . For the lower filter  $\mathbf{B}$ , the reference signal is  $\bar{x}_2$ , and the error signal is  $\bar{x}_1$ . Thus, the orthogonal relationship is expressed as

$$E[\bar{x}_2(k-i)\bar{x}_1(k)]_{\mathbf{B}=\mathbf{B}_{opt}} = 0, \quad i = 0, 1, 2, \dots, M-1, \quad (18)$$

where  $M$  is the number of filter coefficients corresponding to filter  $\mathbf{B}$ . It is important to

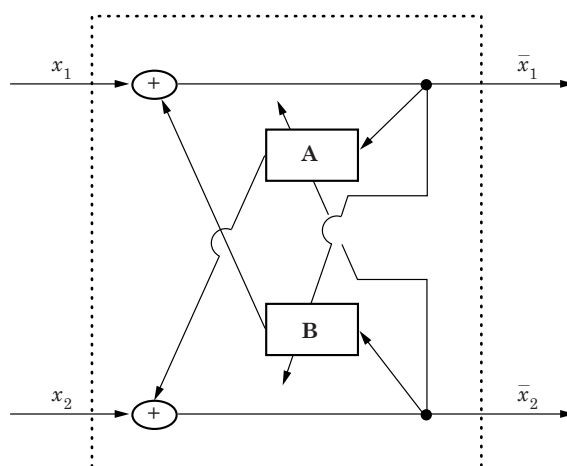


Figure 4. An adaptive decorrelation filter.

note that the degree of decorrelation between the reference signal and the error signal depends on the number of filter coefficients. Ideally, an infinite number of filter coefficients is needed to decorrelate the two reference signals. However, since the objective of applying decorrelation filters is to diagonalize the matrix  $\mathbf{R}$ , it is easy to show that the two transversal filters in the decorrelation filters should have the same number of coefficients, and the number of coefficients  $M$  should be the same as the number of the control filter coefficients.

It should be noted that the first two coefficients  $a_0$  and  $b_0$  in the filters  $\mathbf{A}$  and  $\mathbf{B}$  are redundant, since both of them are trying to achieve

$$E[\bar{x}_2(k)\bar{x}_1(k)] = 0. \tag{19}$$

This is an over-determined case, which gives infinite solutions to  $a_0$  and  $b_0$ . A practical approach is to force either  $a_0$  or  $b_0$  to be zero. Using the LMS algorithm and assuming that first coefficient  $b_0$  is set to be zero, the uncorrelated reference signals  $\bar{x}_1$  and  $\bar{x}_2$  can be obtained as

$$\bar{x}_1(k) = x_1(k) + \sum_{i=1}^M \bar{x}_2(k-i)b_i(k), \quad i = 1, 2, \dots, M-1, \tag{20}$$

$$b_i(k+1) = b_i(k) - \mu \bar{x}_2(k-i)\bar{x}_1(k), \quad i = 1, 2, \dots, M-1, \tag{21}$$

$$\bar{x}_2(k) = x_2(k) + \sum_{i=0}^M \bar{x}_1(k-i)a_i(k), \quad i = 0, 1, 2, \dots, M-1, \tag{22}$$

$$a_i(k+1) = a_i(k) - \mu \bar{x}_1(k-i)\bar{x}_2(k), \quad i = 0, 1, 2, \dots, M-1. \tag{23}$$

The above decorrelation techniques have been reported to achieve signal separation and restoration of the original signals [11, 12]. In these applications, assumptions on the relationship between source signals and input signals have to be made, and also required are some assumptions on the statistical properties of source signals. In the preprocessing, the reference signals are assumed to be wide sense stationary, however, the relationship between noise sources and reference signals is not important. In order to obtain  $K$  uncorrelated reference signals, the Gram-Schmidt process is applied to the reference signals. Firstly, the reference signals  $x_1$  and  $x_2$  are decorrelated through filters  $A_{21}$  and  $B_{21}$ . Then the reference signal  $x_3$  is decorrelated with both  $x_2$  and  $x_1$ . Finally, the reference signal  $x_k$  is decorrelated with all the previous reference signals  $x_1, x_2, \dots, x_{k-1}$  through two sets of filters  $A_{k1}, A_{k2}, \dots, A_{k(k-1)}$ , and  $B_{k1}, B_{k2}, \dots, B_{k(k-1)}$ . The decorrelation structure for  $K$  reference signals is shown in Figure 5. A disadvantage of this structure is that the computation load increases squarely with the increasing number of reference signals, which justifies its application only when the number of reference signals is relatively small.

The correlation matrix  $\bar{\mathbf{R}}$  of decorrelated reference signals is generally not strictly diagonal, but block-diagonal, since each term inside the matrix is a sub-matrix. Although the eigenvalue spread is generally smaller after the preprocessing with the decorrelation filters, it is not guaranteed at every situation. In particular, if the cross-correlation terms are much smaller than the auto-correlation terms in the matrix  $\mathbf{R}$ , the decorrelation preprocess may not improve eigenvalue spread at all. However, if each reference signal itself is orthogonal, which implies that each diagonal sub-matrix inside the matrix  $\mathbf{R}$  is diagonal, the decorrelation process will definitely improve the eigenvalue

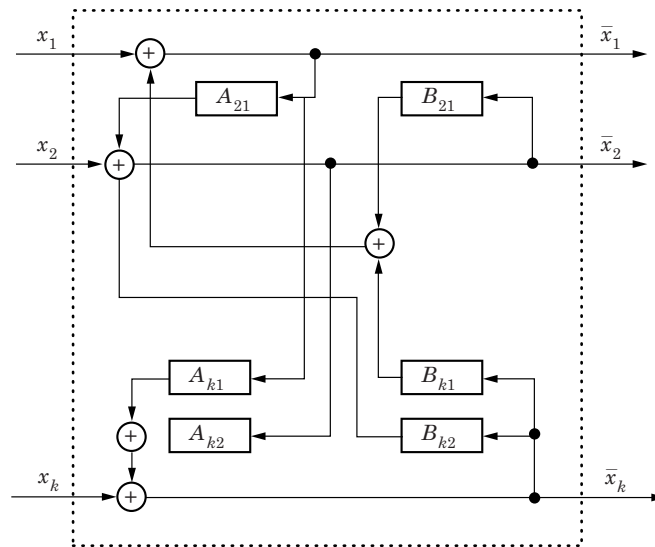


Figure 5. Decorrelation Filter Structure for  $K$  reference signals.

spread. A potential approach to achieve this is to combine the decorrelation process with lattice structure based FIR filters [13, 14] or frequency-domain block algorithm [15, 16].

#### 4. EXPERIMENTAL SETUP

As shown in Figure 6, there are two disturbance sources, one secondary source and one error microphone for the plate system. With the dimension of 0.381 m long and 0.305 m wide, the plate is mounted in a heavy steel frame, which produces negligible

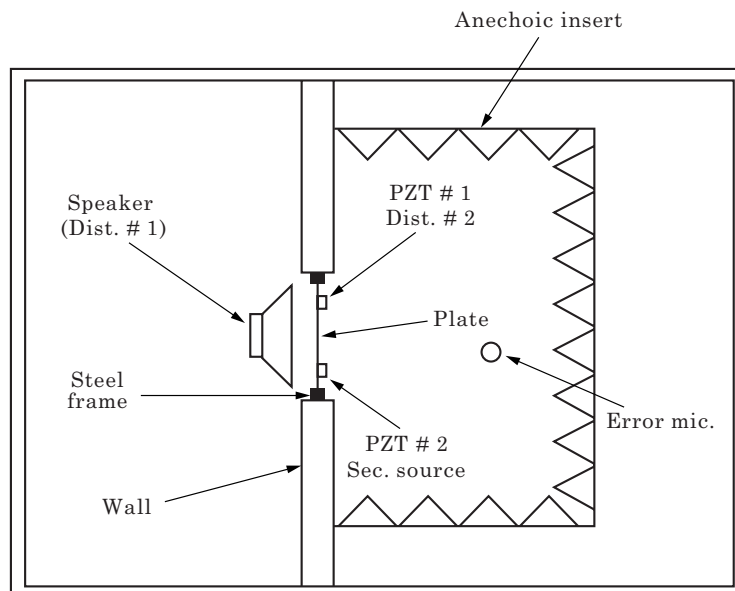


Figure 6. Experimental set-up.



rotation and displacement of the boundary, approximating clamped boundary conditions. The steel frame is further mounted in a rigid wall with one side facing toward a reverberation chamber and the other side toward an anechoic chamber. The plate is excited by two distinctive noise sources; one is the acoustical disturbance from a large speaker, while the other is the structural disturbance from a piezoelectric ceramic transducer (PZT #1) mounted on the plate. The secondary control source acting on the plate is another piezoelectric actuator (PZT #2). The positions of both of the PZTs are selected such that any plate mode of order (4,4) or less can be excited. The error sensor is a microphone located in the direction approximately perpendicular to the center of the plate, but slightly off the center such that the even modes of the plate have relatively small noise contribution, but are still observable and controllable. The goal of the control is to minimize the total radiated sound at the error microphone. The two particular noise sources are chosen in an effort to simulate what happens in an aircraft cabin, which may generate interior noise due to directly applied structural forces as well as acoustical pressure fluctuations acting on it from the exterior.

The block diagram showing the various elements for the experiments is presented in Figure 7. The heart of the system is a TMS320C30<sup>®</sup> DSP board, which is used to implement the preprocessing and control algorithms. The A/D and D/A conversions are carried out through two additional I/O boards, which provide 32 input channels and 16 output channels. The DSP board along with two associated I/O boards are plugged into a PC. A graphical user interface (GUI) running under the host PC is provided to adjust various control parameters and display DSP data. Since the disturbance signals generated within the DSP are digital in nature, they are transformed into analog signals through D/A converters to drive the primary noise sources (speaker and PZT #1). Similarly, the control signal is also transformed into analog signal through D/A converters to drive the secondary source (PZT #2). Since the frequency range for the experiments is selected to be below 400 Hz, all the signals are low-pass filtered so that the frequency components above 400 Hz are negligible in order to avoid alias. In addition, since the signals generated within the DSP have very small power, in order to

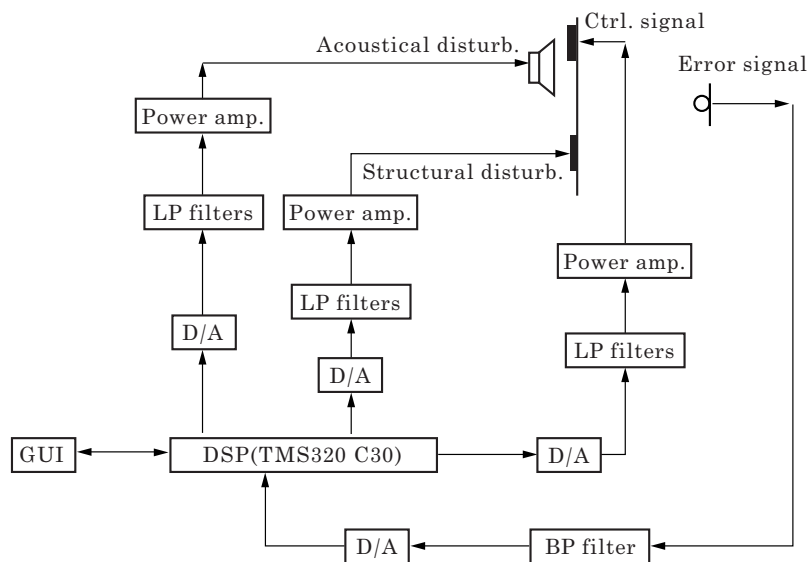


Figure 7. Block diagram of the various elements for the experiments.

drive the speaker and PZTs, they are also fed into power amplifiers. It should be noted that the signal from the error microphone is fed into a high-pass filter to eliminate the dc signal drift.

The controller is based on adaptive FIR filters, and the number of coefficients for each FIR filter is selected to be 128. The error path between the secondary source (PZT #2) and the error sensor is also modelled with a FIR filter, and the same number of coefficients is used. The frequency range of the noise field is selected to be below 400 Hz. These parameters are selected based on the computational limit of the DSP, since increasing the frequency range generally requires more filter coefficients to get satisfactory results, which in turn requires more computations.

Two random signal generators were used to produce two independent noise sources, and the reference signals were obtained indirectly from the two noise sources. The relationship between the reference signals and the noise sources is shown in Figure 8. The first reference signal  $r_1$  is exactly the same as the first noise source signal  $n_1$ . The second reference signal  $r_2$  is the combination of the second noise source  $n_2$  and the first noise source  $n_1$  filtered through a band-pass filter, that is

$$r_1(k) = n_1(k), \quad r_2(k) = C_0^* n_2(k) + n_1(k)H(Z), \quad (24, 25)$$

where  $C_0$  is a constant. The two uncorrelated noise source signals,  $n_1$  and  $n_2$ , are uniformly distributed between  $-1$  and  $1$ . The cut-off frequencies for the band pass filter  $H(z)$  are selected to be 160 and 320 Hz. A FIR filter with four coefficients is used here to implement the band pass filter. The windowing method is adopted to design the band pass FIR filter and the resultant four-coefficient vector is  $\{-1.009, 6.875, 6.875, -1.009\}$ . Thus, the two reference signals in equations (22) and (23) are correlated due to the common contributions from noise source  $n_1$ , and their correlation function can be varied if a different constant  $C_0$  is selected. The decorrelation filters are implemented with fixed Wiener filters instead of adaptive filters since the correlation between the reference signals is time invariant. In this particular case, the requirement for the decorrelation filter is to remove the component in the reference signal  $r_2$ , which is correlated with the reference signal  $r_1$ . The decorrelation filter corresponding to Figure 4 is simply calculated

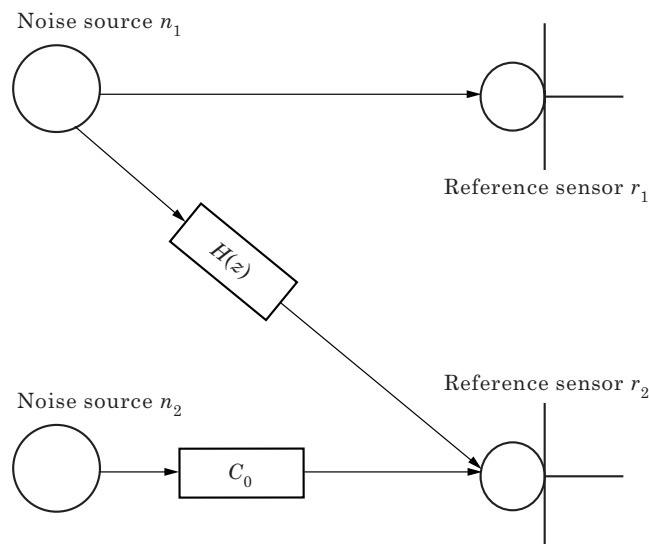


Figure 8. Noise sources and reference sensors.

TABLE 1  
*Eigenvalue spread versus correlation*

$C_0$	Reference signals without decorrelation	Reference signals with decorrelation	Filtered reference without decorrelation	Filtered reference with decorrelation
1.0	17.7	3.2	$8.4 \times 10^6$	$2.3 \times 10^5$
0.5	48.2	3.4	$2.9 \times 10^6$	$3.1 \times 10^5$
0.2	242.5	3.0	$1.1 \times 10^7$	$2.2 \times 10^5$

with the coefficient vector  $\mathbf{A}$  as  $\{1.025, -6.888, -6.863, 1.003\}$ , and the coefficient vector  $\mathbf{B}$  as a zero vector.

Corresponding to each selected constant  $C_0$ , computations are carried out to obtain the correlation matrix  $\mathbf{R}$  for the reference signals, the decorrelated reference signals, the filtered reference signals, and the decorrelated filtered reference signals. Based on the correlation matrix, the corresponding eigenvalue spread is also computed and the results are shown in Table 1. Theoretically, the eigenvalue spread after decorrelation processing should be the same for every  $C_0$ . However, since the expectation value inside the correlation matrix  $\mathbf{R}$  is estimated using 4096 samples, the calculated eigenvalue spread is slightly different from the theoretical value. It is clear that the eigenvalue spread of the reference signals is smaller after it is processed through the decorrelation filter. In fact, the convergence speed is determined by the filtered reference signals instead of the reference signals for the Filtered-X LMS (FXLMS) algorithm. Thus, in order to improve the convergence speed, the eigenvalue spread for the filtered reference signals must get smaller as well. This requirement is indeed satisfied since, although decorrelation is only applied to the reference signals, the correlation between filtered reference signals is also affected. It is also interesting to note that the eigenvalue spread for the filtered reference signals is much larger than that for the reference signals. Such a result can be intuitively viewed from the perspective of a three-dimensional performance surface: the reference signal corresponds to a half-egg-shaped surface, but the error path essentially stretches this performance surface into a very narrow strip resulting in a large eigenvalue spread for the filtered reference signal.

## 5. EXPERIMENTAL RESULTS

If the reference signals are preprocessed through the decorrelation filter, then the FXLMS algorithm is referred to as the DFXLMS algorithm. In order to examine the effect of the decorrelation filter on improving the convergence speed, the conventional FXLMS algorithm was first applied. After letting the controller weight vectors converge for 30 s, the convergence process was frozen. Then the power spectral density of the error signal was measured. Next, the DFXLMS algorithm was also applied, the power spectral density of the error signal was also measured after 30 s of convergence time. The results, shown in Figure 9, indicate that 9.0 dB noise reduction was achieved with the DFXLMS algorithm, while only 5.3 dB noise reduction was achieved with the conventional FXLMS algorithm.

In order to measure the learning curve, the convergence process of the FXLMS algorithm or the DFXLMS algorithm was started with a small convergence parameter, and values of the error signal power at 5, 10, 15, 25... and 360 s were measured. These values representing the power of the error signal form the learning curves, as shown in

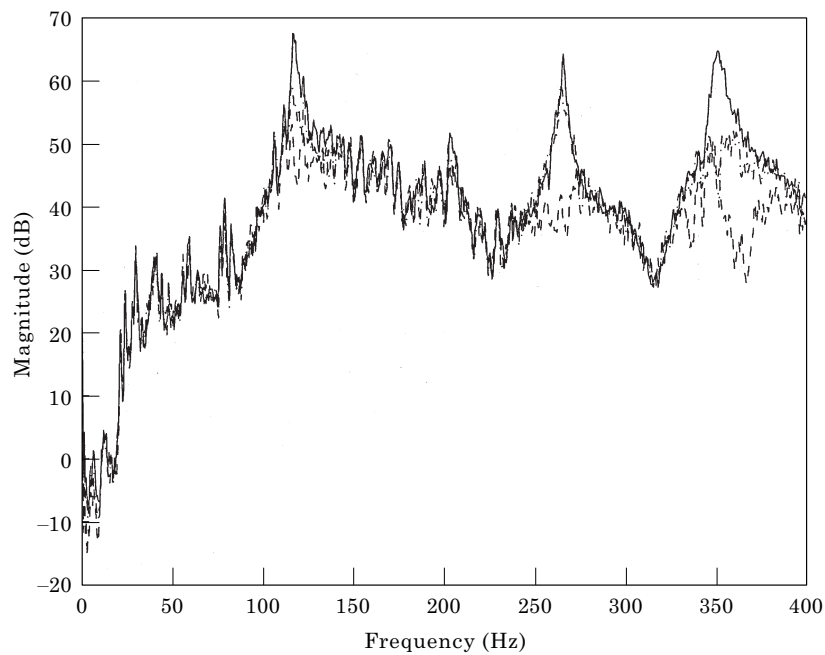


Figure 9. Spectrum of error signal after 30 s convergence time: —, before control; ---, without decorrelation filter; -·-·, with decorrelation filter.

Figure 10. The results indicate that the DFXLMS algorithm converges about three times faster than the FXLMS algorithm and the improvement of the convergence speed is in the same magnitude as the improvement of the corresponding eigenvalue spread. It is

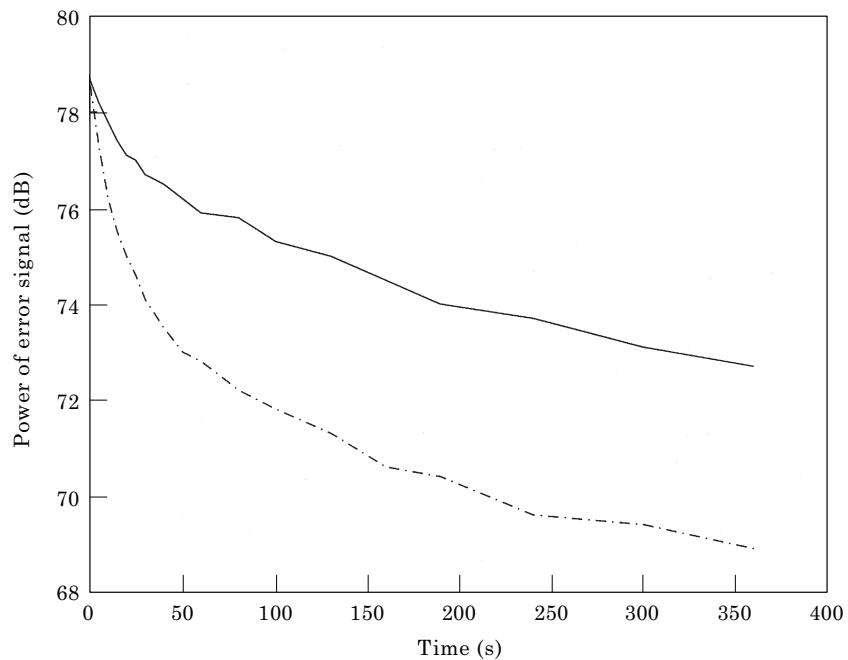


Figure 10. Comparison of learning curves based on experiment: —, without decorrelation; -·-·, with decorrelation.

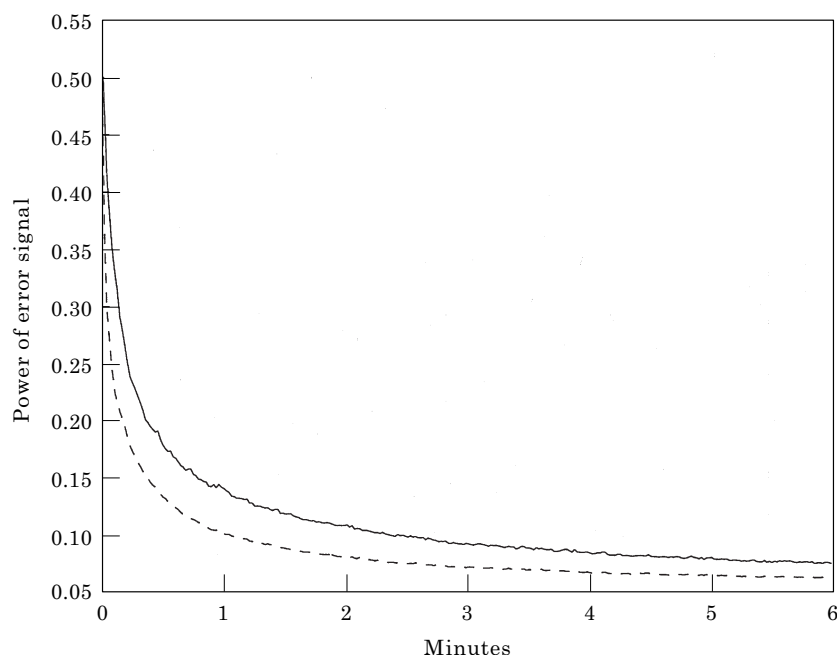


Figure 11. Comparison of learning curves based on simulation: —, without decorrelation filter; ---, with decorrelation filter.

interesting to note that the error signal power for the DFXLMS is still larger than that for the FXLMS algorithm after 360 s. This is mainly due to the very long convergence time needed for the error signals to reach steady state. However, various measurement errors or distortions (e.g., A/D and D/A conversion, non-linearity, finite precision) introduced in the experiment may also play a role since a larger condition number causes control performance to be more sensitive to those measurement distortions.

In order to investigate the impact of measurement errors, a simulation based on the same experimental set-up was carried out using the approach outlined in the companion paper. The frequency response functions of the two primary paths (from the speaker through the plate to the error microphone and from the PZT #1 to the error microphone) and one error path (from the PZT #2 to the error microphone) were measured with a B&K 2032 digital signal analyzer. The frequency response functions were fitted with FIR filters using the least square method [17]. Based on the FIR models, the learning curves of the two algorithms can be obtained through calculation. The results, shown in Figure 11, show the same tendency that the convergence speed of the DFXLMS algorithm is about three times as fast as that of the traditional FXLMS algorithm. However, after 6 min of convergence, the power of the error signal with the DFXLMS algorithm is very close to that with the FXLMS algorithm. Since the simulation is free from various measurement errors and noise caused by A/D, D/A converters, transducers, non-linear behaviour and many other ANC elements, the simulation results of Figure 11, when compared to the corresponding experimental results of Figure 10, tend to suggest that the DFXLMS algorithm has improved attenuation when there is distortion of the measured signals. This aspect, which for brevity is not investigated in detail in the present paper, will be the topic of a future investigation.

## 6. CONCLUSION

The optimum solution of a multiple reference feedforward active noise control system has been obtained in the time domain. It was particularly noted that if the reference signals are correlated, the corresponding system would be ill-conditioned, which results in slow convergence speed and high sensitivity to measurement errors. A decorrelation approach has been constructed for preprocessing reference signals based on the Wiener filter theory and Gram–Schmidt orthogonalization theorem. Experiments based on sound transmission through a vibrating plate have been conducted, and the results demonstrate the effectiveness of the decorrelation approach to improve both the convergence speed and steady state error.

## ACKNOWLEDGMENTS

The authors gratefully acknowledge the support of this work by the office of Naval Research under the Grant ONR N00014-94-1-1140; Dr Kam Ng, Technical Monitor.

## REFERENCES

1. C. R. FULLER and A. H. VON FLOTOW 1995 *IEEE Control Systems December*, 9–19. Active control of sound and vibration.
2. P. A. NELSON and S. J. ELLIOT 1992 *Active Control of Sound*. San Diego: Academic Press.
3. Y. TU and C. R. FULLER *Journal of Sound and Vibration* (submitted). Multiple reference feedforward active noise control, part I: analysis and simulation of behavior.
4. A. B. E. MASATO, GUO-YUE CHEN and TOSHIO SON 1993 *Proceedings of Inter-Noise*, 759–762. A method to increase the convergence speed by using uncorrelators in the active control of multiple noise sources.
5. P. D. HILL and W. B. MIKHAEL 1990 *Proceedings of the 32nd Midwest Symposium on Circuits and Systems*, Volume 1, **P.2 vol. 1266**, 605–608. A new formulation of the multiple reference adaptive noise cancellation filter.
6. R. B. WALLACE and R. A. GOUBRAN 1992 *IEEE International Symposium on Circuits and Systems*, Volume 2, **P.6 vol. 3028**, 525–528. Parallel adaptive filter structures for acoustic noise cancellation.
7. C. M. HEATWOLE and R. J. BERNHARD 1996 *Noise Control Engineering* **44**, 35–43. Reference transducer selection for active control of structure-borne road noise in automobile interiors.
8. S. M. KUO and D. R. MORGAN 1996 *Active Noise Control Systems: Algorithms and DSP Implementations*. New York: Wiley.
9. S. HAYKIN 1991 *Adaptive Filter Theory*. Englewood Cliffs, NJ: Prentice-Hall; second edition.
10. D. S. WATKINS 1991 *Fundamentals of Matrix Computations*. New York: Wiley.
11. E. WEINSTEIN, M. FEDER, and A. V. OPPENHEIM 1993 *IEEE Transaction on Speech Audio Processing* **1**, 405–413. Multi-channel signal separation by decorrelation.
12. S. GERVEN and D. COMPERNOLLE 1995 *IEEE Transaction On Signal Processing* **43**, 1602–1612. Signal separation by symmetric adaptive decorrelation: stability, convergence, and uniqueness.
13. J. MAKHOUL 1994 *IEEE Transaction on Acoustics, Speech and Signal Processing ASSP-26*, 304–313. A class of all-zero lattice digital filters.
14. L. J. GRIFFITHS 1979 *Proceedings of International Conference on Acoustics, Speech, and Signal Processing*, 925–928. Adaptive structures for multiple-input noise canceling applications.
15. J. J. SHYNK 1992 *IEEE Signal Processing Magazine* **9**, 14–37. Frequency-domain and multi-rate adaptive filters.
16. Q. SHEN and A. S. SPANIAS 1992 *Proceedings of 2nd International Congress on Recent Developments in Air- & Structure-Borne Sound and Vibration, Auburn, Al* 353–360. Time and frequency domain X Block LMS algorithms for single channel active noise control.
17. A. A. GIORDANO and F. M. HSU 1985 *Least Square Estimation With Applications to Digital Signal Processing*. New York: Wiley.